VIDEO IMAGE PROCESSING TO CREATE
A SPEED SENSOR

by

D.J. Dailey and L. Li
ITS Research Program
College of Engineering, Box 352500
University of Washington
Seattle, Washington 98195-2500

Washington State Transportation Center (TRAC)
University of Washington, Box 354802
University District Building
1107 NE 45th Street, Suite 535
Seattle, Washington 98105-4631

Washington State Department of Transportation
Technical Monitor
Bill Legg

Prepared for

April 2000

TECHNICAL REPORT STANDARD TITLE PAGE

1. REPORT NO. WA-RD 465.1	2. GOVERNMENT ACCESSION NO.	3. RECIPIENT'S CATALOG NO.	
4. TITLE AND SUBTITLE Video Image Processing to Create a Speed Sensor		5. REPORT DATE April 2000	
		6. PERFORMING ORGANIZATION CODE	
7. AUTHOR(S) D.J. Dailey, L. Li		8. PERFORMING ORGANIZATION REPORT NO.	
9. PERFORMING ORGANIZATION NAME AND ADDRESS Washington State Transportation Center (TRAC) University of Washington, Bx 354802 University District Building; 1107 NE 45th Street, Suite 535 Seattle, Washington 98105-4631		10. WORK UNIT NO.	
		11. CONTRACT OR GRANT NO. Agreement T9903, Task 75	
12. SPONSORING AGENCY NAME AND ADDRESS Washington State Department of Transportation Transportation Building, MS 7370 Olympia, Washington 98504-7370		13. TYPE OF REPORT AND PERIOD COVERED Research report	
		14. SPONSORING AGENCY CODE	
15. SUPPLEMENTARY NOTES This study was conducted in cooperation with the U.S. Department of Transportation, Federal Highway Administration.			

16. ABSTRACT

   Image processing has been applied to traffic analysis in recent years with different goals. In this report, a new approach is presented for extracting vehicular speed information, given a sequence of real-time traffic images. We extract moving edges and process the resulting edge information to obtain quantitative geometric measurements of vehicles. This differs from existing approaches because we use simple geometric relations obtained directly from the image instead of using reference objects to perform camera calibrations. Our method allows the recovery of the physical descriptions of traffic scenes without explicit camera calibration.

   In this report, extensive experiments using images from active TMS Transportation Management System (TMS) freeway cameras are reported. The results presented in this report demonstrate the validity of our approach, which requires neither direct camera control nor placement of a calibration object in the environment. We further argue that it is straightforward to extend our method to other related traffic applications.

17. KEY WORDS Video image processing, CCTV cameras, speed sensor, moving edge detection	18. DISTRIBUTION STATEMENT No restrictions. This document is available to the public through the National Technical Information Service, Springfield, VA 22616		
19. SECURITY CLASSIF. (of this report) None	20. SECURITY CLASSIF. (of this page) None	21. NO. OF PAGES	22. PRICE

Disclaimer

The contents of this report reflect the views of the authors, who are responsible for the facts and accuracy of the data presented herein. This document is disseminated through the Transportation Northwest (TransNow) Regional Center under the sponsorship of the U.S. Department of Transportation UTC Grant Program and through the Washington State Department of Transportation. The U.S. government assumes no liability for the contents or use thereof. Sponsorship for the local match portion of this research project was provided by the Washington State Department of Transportation. The contents do not necessarily reflect the official views or policies of the U.S. Department of Transportation, the Washington State Department of Transportation, or the Federal Highway Administration. This report does not constitute a standard, specification, or regulation.

Abstract

Image processing has been applied to traffic analysis in recent years, with different goals. In this report, a new approach is presented for extracting vehicular speed information, given a sequence of real-time traffic images. We extract moving edges and process the resulting edge information to obtain quantitative geometric measurements of vehicles. This differs from existing approaches because we use simple geometric relations obtained directly from the image instead of using reference objects to perform camera calibrations. Our method allows the recovery of the physical descriptions of traffic scenes without explicit camera calibration. In this report, extensive experiments using images from active TMS (Transportation Management System) freeway cameras are reported. The results presented in this report demonstrate the validity of our approach which requires neither direct camera control nor placement of a calibration object in the environment. We further argue that it is straightforward to extend our method to other related traffic applications.

Contents

List of Figures

1 Introduction

In recent years, image processing has been applied to the field of traffic research with goals that include queue detection, incident detection, vehicle classification, and vehicle counting [1, 2, 3, 4, 5, 6, 7].

This report explicitly recognizes that speed is an important parameter in traffic analysis. Relatively few efforts have attempted to measure speed by using video images from uncalibrated cameras. Some preliminary research on pixel speed estimation in images appears in Soh et al [6] and Picton [8]. A review of the literature on physical speed estimation shows that almost all of the algorithms involve some man-made reference information. For example, Worrall et al [9] describes an interactive tool for performing camera calibration. In this interactive application, an operator first identifies vanishing points from parallel road marks and then places a rectangular grid on the image for calibration. Dickinson and Waterfall [10] and Ashworth et al [11] make speed measurements from the known physical distance between two detection windows placed on the road image. Similarly, several other papers [12, 13] suggest estimating speed by first placing two detection lines (separated by a known distance) and then measuring travel times between the lines. Houkes [14] determined four reference points to form a rectangle before taking the off-line measurements. In that case, the camera had to remain in the same position during all measurements for the process to be valid.

In this research, we assumed that we had no control over camera movements and thus could not directly obtain information such as camera focus, tilt, or angle. We further assumed that the camera parameters could change any time without our knowledge. In our project, we were monitoring congested freeways and had neither the ability nor the authority to set permanent marks on the road.

We believe on-line calibration is a necessary step in using the large, installed base of TMS cameras. We propose that exact calibration is not necessary to estimate speed using our

algorithm; instead, we use information inherently available in the image. We focus on a 1-D geometry for the traffic on the road. Using a car length distribution from our previous research [15], we propose a novel method that extracts scaling signatures and computes the speed distribution on the basis of the geometric relationships in the image.

1.1 ASSUMPTIONS

To clarify the problem presented here, we made several assumptions in our work:

a) Finite speed [16]: The speed of a vehicle has both physical and legal limits.

b) Movement is smooth [16]: No sudden changes of directions are expected between frame intervals (330ms).

c) Motion is constrained to the road plane [17], and thus we are posing camera calibration as a 1-D geometry problem.

In this work, we used 320x240 gray-scale images at a frame rate of 3 frames per second (fps). These are demonstrated to be adequate for reliable analysis, as well as being small enough to allow efficient processing.

1.2 REPORT OVERVIEW

Our algorithm for speed extraction first applies a series of operators to single images to create a set of enhanced images. We then use this set of enhanced images to create a speed estimation algorithm. In this report, we first describe the single image operations and then present the overall algorithm as applied to a group of images. Chapter 2 introduces major procedures for each single image. These consist of a preprocessing step, a moving-edge detection step, a morphological operation step, and a convex hull and bounding box extraction step. In Chapter 3, we discuss geometric relation analysis, as well as distance and speed estimation algorithms for an image sequence. Chapter 4 presents the field trials, experimental results, and discussion. In Chapter 5, we present conclusions about the effectiveness of the algorithm.

2 Single Frame Processing

The single image processing steps are shown in Figure 2.1. These steps include preprocessing, moving edge detection, morphological operations, and convex hull and bounding box extraction. The next section describes details of the pre-processing under the assumptions presented earlier.

```
                    ┌─────────────────────────┐
                    │   Preprocessing         │
                    │  (Median filtering)     │
                    └─────────────────────────┘
                                │
                    ┌─────────────────────────┐
                    │  Moving-edge detection  │
                    │ Inter-differencing & Sobel │
                    └─────────────────────────┘
                                │
                    ┌─────────────────────────┐
                    │ Morphological operation │
                    │   (dilation & erosion)  │
                    └─────────────────────────┘
                                │
                    ┌─────────────────────────┐
                    │ Convex Hull & bounding  │
                    │    box extraction       │
                    └─────────────────────────┘
```
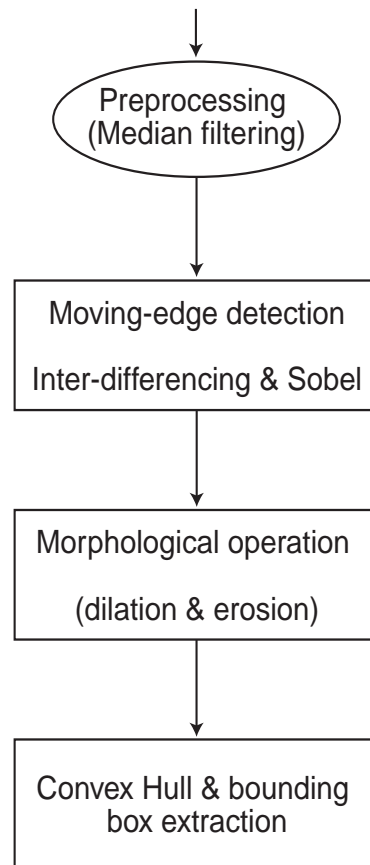
Figure 2.1 Image processing flow for a single image

2.1 PREPROCESSING

The traffic images have a noise component from several interference sources. The types of noise include the following [18]:

1) Salt-and-pepper noise, which occurs when an image is coded and transmitted over a noisy channel or degraded by electrical sensor noise, as in video cameras.

2) Convolutional noise (blurring), which produces images that are degraded by lens mis-focus, motion, or atmospheric turbulence, such as adverse weather conditions.

Both noise sources contribute to high-frequency noise components. In our process, median filtering is used to reduce this high-frequency noise. It preserves the edge information required by our algorithm. Edges are a key image feature, as they remain prominent despite the variations in the traffic scene's ambient lighting. Our median filter uses a 3x3 kernel to remove high frequency noise from the image.

The 3x3 kernel moves row by row, pixel by pixel. A pixel is regarded as the center of the 3x3 window. The median value of the set of nine pixels in the 3x3 neighborhood is used as the new filtered value of the pixel at the center. This way, impulse noise with extreme values can be suppressed. Since the total area in our process is fixed in advance, locating the median value is fast. It is the fifth value in the sorted array [19].

The next section describes the moving edge detection module of our algorithm. The algorithm uses the images preprocessed by the median filtering just presented.

2.2 MOVING-EDGE DETECTION

Moving edge detection is applied to extract the moving parts from a complex background in an image sequence. The static background is then deleted to locate the moving objects.

2.2.1 Sobel Edge Detector

Let $I(i,j)$ denote the pixel value being processed. Its neighbors are considered to determine whether it is on an edge or not. Usually a 3x3 or 5x5 neighbor window is used for

one pixel. In our work, a 3x3 window is used for processing, as shown in the matrix below.

I_3	I_2	I_1
I_4	$I(i,j)$	I_8
I_5	I_6	I_7

For the pixel $I(i,j)$, the eight neighbors are I_1 through I_8.

The Sobel edge magnitude is computed is [20] as

$$I_s(i, j) = (u^2 + v^2)^{1/2},$$ (1)

where

$$u = (I_5 + 2I_6 + I_7) - (I_1 + 2I_2 + I_3),$$ (2)

and

$$v = (2I_8 + I_1 + I_7) - (I_3 + 2I_4 + I_5).$$ (3)

The gradient is computed as

$$G_s(i, j) = tan^{-1}(u / v).$$ (4)

The above computational process moves a 3x3 window with the current pixel as the window center. After the magnitude is obtained, a threshold can be used to determine which pixel is on an edge. If the Sobel magnitude is below the threshold, the pixel will be discarded. This means that the magnitude response is not strong enough to claim an edge point. The selection of an appropriate threshold is dependent on the content of the images.

An example is shown in Figure 2.2. We assert that most of the edges are detected by Sobel edge detection.

8

2.2.2 Moving Edge Detection

In previous work by Gil [21], moving objects were segmented from the traffic background with a motion detection algorithm based on a multi-resolution relaxation. This resulted in a set of coarse binary masks for each vehicle. A refinement process was then applied to obtain a more accurate description. In multi-resolution relaxation, both the starting and ending resolution need to be selected on the basis of engineering judgment. Fathy and Siyal [2] present a window-based edge detection method that combines morphological edge detectors and a median filtering. However, their process [2] requires the user to pre-place all the detection windows at the key regions across the lanes, and therefore the user needs to have detailed knowledge of the road. Kudo [22] applies a one-dimensional gradient operation to a sub-region with a window along the road, which falls into the same category.

Original image
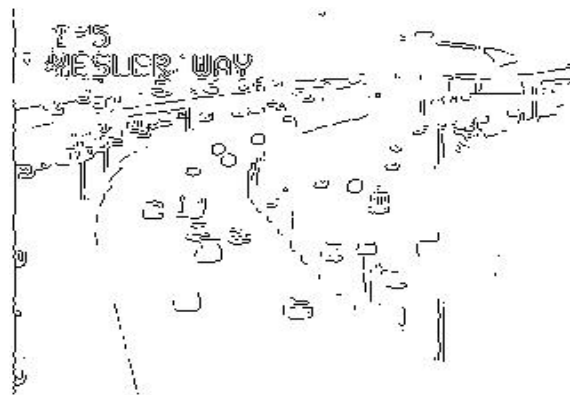
Sobel edge image

Figure 2.2 Sobel edge detection

In this process, we use image differencing to extract motion information. There are two basic differencing methods in the literature: 1) background differencing and 2) interframe differencing. In background differencing, a reference frame that contains no moving vehicles is subtracted from each frame. In real world applications, where the ambient lighting varies rapidly, the reference frame needs to be updated regularly to reflect the current background and to provide reliable segmentation. This reference frame can be obtained by either grabbing a frame when no vehicles are presented or by multi-frame accumulation [23]. Several methods are suggested by Fathy and Siyal [2] and Koller et all [17] to update the background image. However, these methods are slow and computationally expensive and thus cannot meet real-time processing requirements. Furthermore, on congested freeways (the domain of interest) it is difficult to obtain images with no vehicles that match the present light level. Therefore, to mitigate these problems, we adopt the inter-frame differencing method to eliminate the complex background and detect the moving vehicles.

Cai [23] used forward and backward image differencing and then extracted common regions corresponding to the moving areas. Instead of extracting regions, Vieren [24] proposed a method to combine inter-frame differencing and a differential operator to extract moving edges. In our process, we combine inter-frame differencing with the Sobel edge detector to extract the moving edges. To emphasize the movement signature, we use three sequential images and process each image relative to its previous and subsequent images. In this way, we separate the movement from the static background.

Our algorithm is applied to three images: the previous temporal image (I_p), the current image of interest (I_c), and the next temporal image (I_n):

$$Edge\_image = Sobel(I_p - I_c) \cap Sobel(I_n - I_c) \ .$$

(5)

That is:

1) Take the difference between the previous image I_p and the
   current image I_c.
2) Take the difference between the next image I_n and the
   current image I_c.
3) Sobel edge operators are applied to these two different
   images to get two edge images.
4) Compare the magnitudes of all edge pixels in the two edge
   images resulting from the Sobel edge operator with a
   magnitude threshold. If the magnitude of a pixel is less
   than the threshold, then it is set to be 0. Otherwise, it
   is set to be 1. This produces two binary edge images.
5) Create the intersection of the two binary edge images.
   Extract common moving edges present in the original current
   image, I_c.

This process produces an edge image for the current image of interest from which we

will extract individual vehicle information in the next chapter.

Figure 2.3 A typical sequence

Example images for the above process are shown in Figures 2.3, 2.4, 2.5, and 2.6. Figure 2.3 shows three original successive frames in an image sequence. Figure 2.4 shows the edge image of the difference image between the first two frames. Figure 2.5 shows the edge image of the difference image between the second and third frames. Figure 2.6 shows the final moving edge image. Almost all of the moving edges are extracted successfully.

Figure 2.4 Sobel edges in the difference image between the first two frames

Figure 2.5 Sobel edges in the difference image between the second and third frames
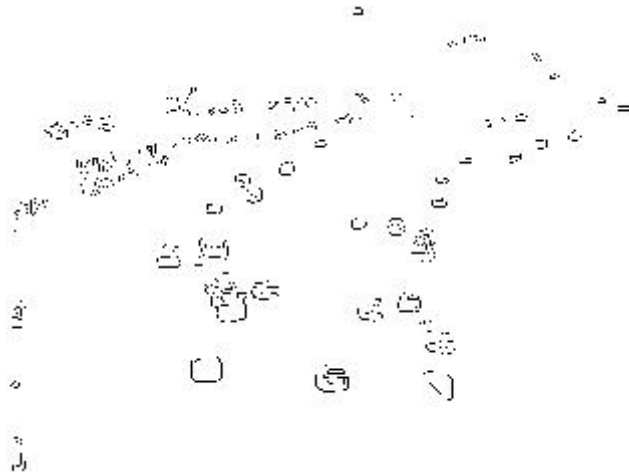
Figure 2.6 Moving edges

2.3 MORPHOLOGICAL OPERATION TO OBTAIN MOVING BLOBS

In the moving edge image just described, there are always gaps along the edges. To obtain a profile of the vehicle, we need to enhance the moving edges. This enhancement uses the morphological operators dilation and erosion with an appropriate structural element. The result of sequentially applying dilation and erosion [25] is to remove specific image features smaller than the structural element without affecting the large features of interest.

Dilation and erosion are two basic morphological operations, which will be discussed first. Dilating an object is to translate all its points with regard to a structural element followed by union operation. On the other hand, eroding an object is to translate all its points first by using a structural element and then to conduct the intersection operation to get the final result. This way, dilation expands an object and erosion shrinks it by the size of the specified structural element.

Images are dilated with the max operation. They are eroded with the min operation. A structural element of N by N is used to define the *max* or *min* operation regions. To process an image pixel, the region containing the pixel of interest and its (N-1) by (N-1) neighboring pixels is processed, and the maximum or the minimum value is obtained.

That is, for an image matrix with *m* by *n*, and a given element size *N*,

```
1)   sort the pixel values in the N by N neighborhood
2)   put the maximum in the dilation image matrix
3)   put the minimum in the erosion image matrix.
```

Since we are processing binary images, the above sorting process can be simplified to test whether the pixel value is 1 or 0. In this way, the operations are very fast.

The selection of the size of the structural element *N* depends on the range of the size of the vehicles of interest and the range of distance between the vehicles. For example, a vehicle smaller than the structural element in the image will be removed by erosion. On the other hand, several vehicles close to each other will be merged to a single blob after dilation. While our goal is to extract as many vehicles as possible, we do not require every vehicle in the image to be identified for our algorithm to accurately estimate speed. Using morphological operations, some vehicles will be removed by erosion because of their small size in the image (these have been deemed too small to be useful in speed estimation) or will be merged by dilation because of their proximity (these have been deemed inappropriate because of possible occlusion effects).

Figures 2.7 and 2.8 show some morphological examples. Figure 2.7 shows the result of dilation operation. Different structural element sizes (3x3 and 4x4) are used. Observe that dilation with larger sized structural elements will make some blobs merge together. Figure 2.8 shows erosion operations. Erosion with larger sized structural elements causes some vehicles to disappear from the image.

14
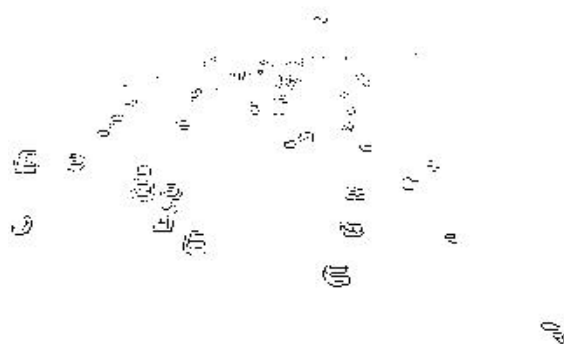
Original Binary image

After dilation by a 3x3 structural element

After dilation by a 4x4 structural element

Figure 2.7 Dilation examples
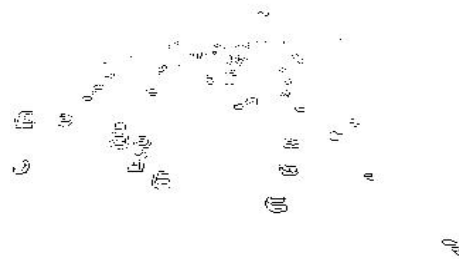
(1) original binary image

(2) After erosion by a 3x3 structural element

(3) After erosion by a 4x4 structural element

Figure 2.8 Erosion examples

The result of sequentially applying dilation and erosion [25] is to remove specific image features smaller than the structural element without affecting the large features of interest. An example is shown in Figure 2.9, where an image is first dilated and then eroded by the same 3x3 structural element.

Original binary image
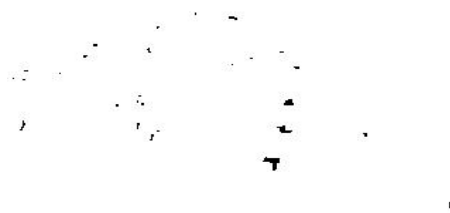
After dilation

After erosion

Figure 2.9 Dilation followed by erosion

At this stage, the image of interest has been enhanced to emphasize the moving vehicles that appear as blobs in the resulting image.

2.4 VEHICLE PROFILE APPROXIMATION

2.4.1 Convex Hull Extraction

After the application of morphological operators above, moving edges are filled and appear as solid moving "blobs." To characterize the blobs, we use a convex hull to approximate the contour of the vehicles. In many cases, a convex hull is a good approximation of the projection of a car [21, 17].

In the image produced by the procedure in the previous section, the background is full of 0s, and only points inside and along the contours of the blob are of value 1. We select the contour points by searching each scanline to find the rightmost or leftmost end of a blob.

Not all contour points selected by this method will belong to the convex hull. Therefore, we need to select those points that are actually on the hull. Koller [17] proposed a convex hull extraction method that is suitable for our purpose. The procedure is to define a convex hull point, $P_2(x_2, y_2)$, by its location related to its preceding point, $P_1(x_1, y_1)$, and following point $P_3(x_3, y_3)$. A threshold T is used to determine the associated orientation of these three points, where

$$T = \begin{vmatrix} x_1 & y_1 & 1 \\ x_2 & y_2 & 1 \\ x_3 & y_3 & 1 \end{vmatrix}.$$

(6)

A positive value of T indicates that those three points are in counter-clockwise order along the contour. A negative T value indicates that they are in clock-wise order.

This algorithm is used to efficiently obtain all the points on the convex hull, as shown in the following description:

```
1) If contour point P₂ is on the left side of the contour, T is
   computed to check whether it is positive (counter-
   clockwise).  If so, P₂ is regarded as being on the convex
   hull.  If not, P₂ does not belong to the hull.
2) Similarly, if P₂ is on the right side of the contour, T is
   computed to check its sign.  Now, contrary to the above
   left-side case, if T is positive, it means P₂ is not on the
```
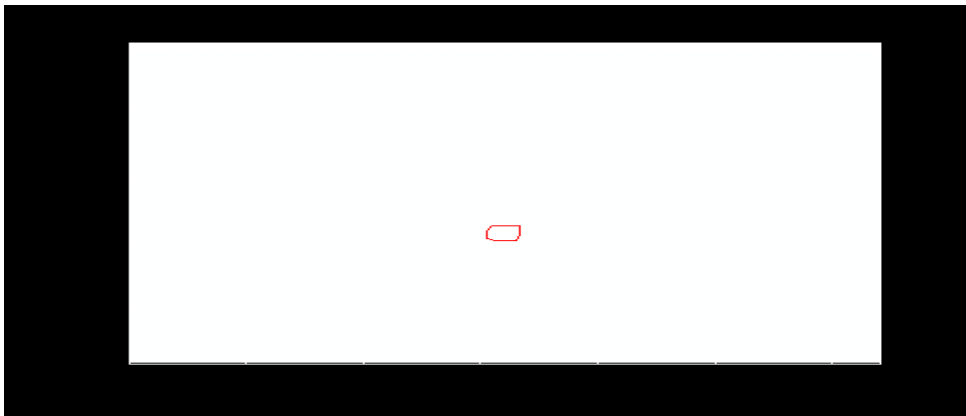
```
convex hull.   If T is negative (clockwise), P₂ belongs to
the hull and should be retained.
```

Figure 2.10 shows an example where a convex hull is extracted by using the above method.

Moving blobs for convex hull extraction

Convex Hull for one blob

Figure 2.10 Convex hull extraction example

2.4.2 Bounding Box Extraction

To obtain scaling information directly from the image rather than using explicit camera calibration, we exploit the known geometric relationships in the images. We do this

by constructing a bounding box to enclose the convex hull. This bounding box is used to isolate the area of interest in the image and is similar to window (or key region) processing described by Fathy and Siyal [26] and Stewart et al [27]. However, unlike window processing, we are only interested in looking for some simple geometric relations inside the box.

To obtain the bounding box from the convex hull with vertices x_i and y_i, the algorithm, as seen in Figure 2.11, is:

```
1) Arrange all the xᵢ values as an array and find the minimum
   and maximum.
2) Do the same for all yᵢ values.
3) The resulting box is the rectangle with vertices (counter-
   clockwise order):
   (min_xᵢ, min_yᵢ)(max_xᵢ, min_yᵢ)(max_xᵢ, max_yᵢ)
   (min_xᵢ, max_yᵢ).
```

(min_x_i, max_y_i) (max_x_i, max_y_i)

(min_x_i, min_y_i) (max_x_i, min_y_i)
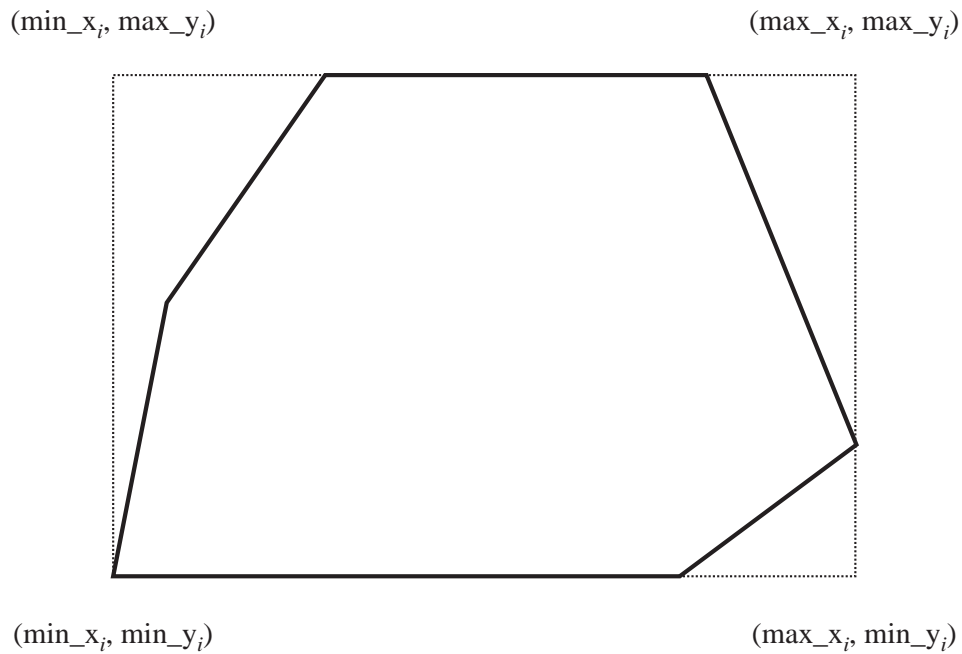
Figure 2.11 Bounding box enclosing a convex hull

This procedure is applied to each image in an image sequence, and we obtain a series of convex hulls and bounding boxes that will be used to estimate the real travel distance and speed, as covered in the next chapter.

Figure 2.12 shows an example of extracting the bounding box from a convex hull.
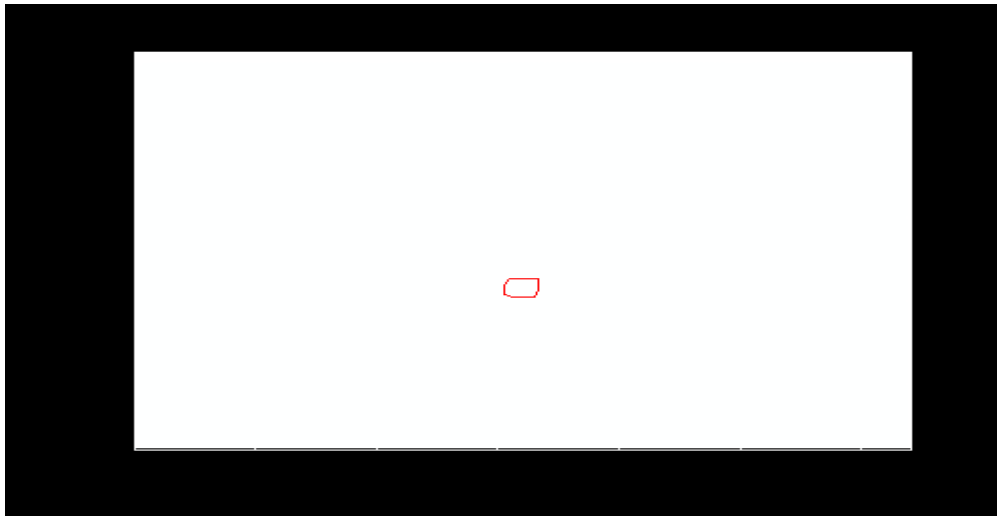
Convex Hull for bounding box extraction
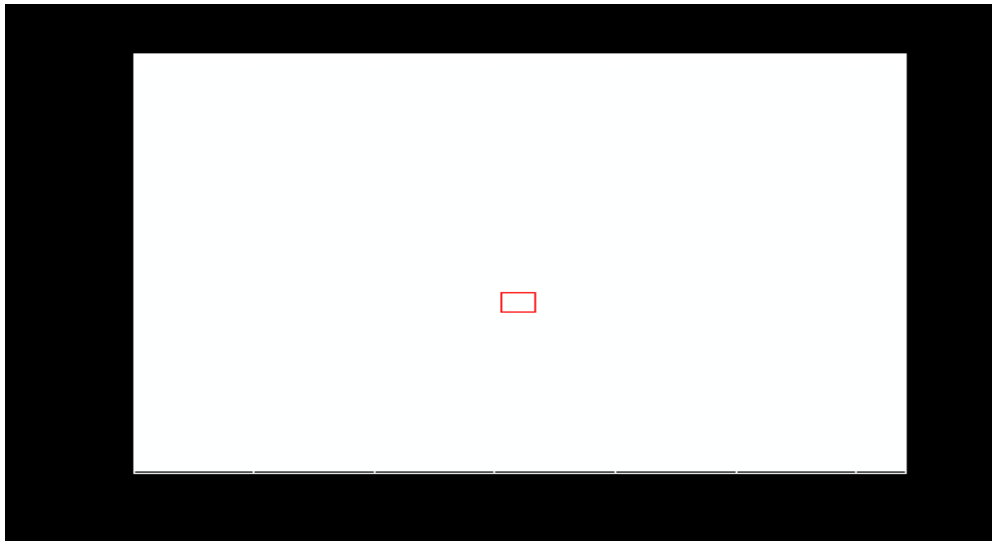
Bounding box extracted

Figure 2.12 Bounding box extraction

3 Geometric Analysis and Speed Estimation From an Image Sequence

The result from Chapter 2 is a series of convex hulls and bounding boxes. This chapter describes utilizing the geometric features and this series of hulls and blobs for distance and speed computation.

To estimate speed, we first obtain the direction of motion of each vehicle and then compute the best fit line through the centroids of the convex hulls found in a series of images and associated with a single vehicle. A threshold on the correlation coefficient [28] for the centroids is used as the colinearity criterion to identify a single vehicle track. The best fit line for the direction of travel is used to obtain the pixel length of the vehicle, and we exploit a simple triangular relationship in the bounding box to get the pixel length of the vehicle, which is then used to compute the scale information in the images. Ground truth distance is estimated by using scale information along the direction of motion, and these distances, with the frame rate of the video sequence, are used to estimate speed.

3.1 DIRECTION OF MOTION: α

We assume that the vehicles make no sudden changes in directions between successive video frames. This assumption allows us to track individual vehicles through successive frames. We identify a single vehicle track by requiring that the centroids of the convex hull be colinear in successive frames, as shown in Figure 3.1. The linear regression correlation coefficient r for least square straight line fitting, as presented by Bevington [28], is the criterion for determining the colinearity of centroids.

From experiments, we claim that we are able to identify a single vehicle in a succession of images if the colinearity of the centroids produces a linear regression correlation coefficient r greater than 0.90, where

$$r = \frac{n\sum_{i-1}^{n} x_i y_i - \sum_{i-1}^{n} x_i \sum_{i-1}^{n} y_i}{\sqrt{n\sum_{i-1}^{n} x_i^{2} - \left(\sum_{i-1}^{n} x_i\right)^{2}} \sqrt{n\sum_{i-1}^{n} y_i^{2} - \left(\sum_{i-1}^{n} y_i\right)^{2}}}, \qquad (7)$$

and x_i and y_i are the coordinates of convex hull centroids.
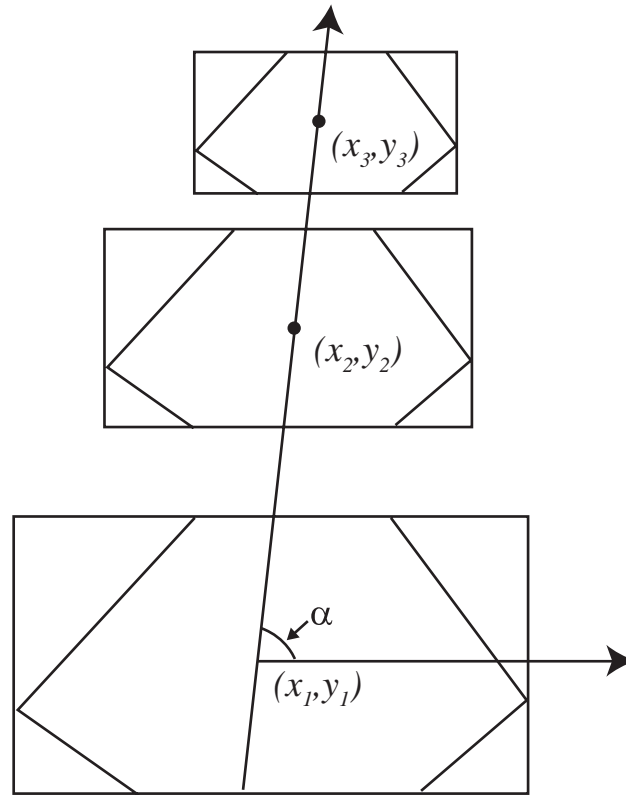
Figure 3.1 Colinearity of convex hull centroids

3.2 GEOMETRIC RELATION INSIDE THE BOUNDING BOX

To get the scale information from the images, we exploit the triangular relationship within the bounding box, as shown in Figure 3.2. The pixel length, *L_pixel*, of a vehicle is estimated along the best fit line (*L*) indicating the direction of travel. It is estimated to be the length of the cord along the best fit line that intersects the bounding box.

$$L\_pixel = \frac{box\_width}{\sin \alpha} \quad . \tag{8}$$

Figure 3.2 Triangular relation

To map the pixel length to ground truth vehicle lengths, we use the empirical vehicle length distribution shown in Figure 3.3 [15]. This allows us to readily obtain the ratio of the physical length, *L_physical*, and the pixel length, *L_pixel*, which is the scale factor *s*,

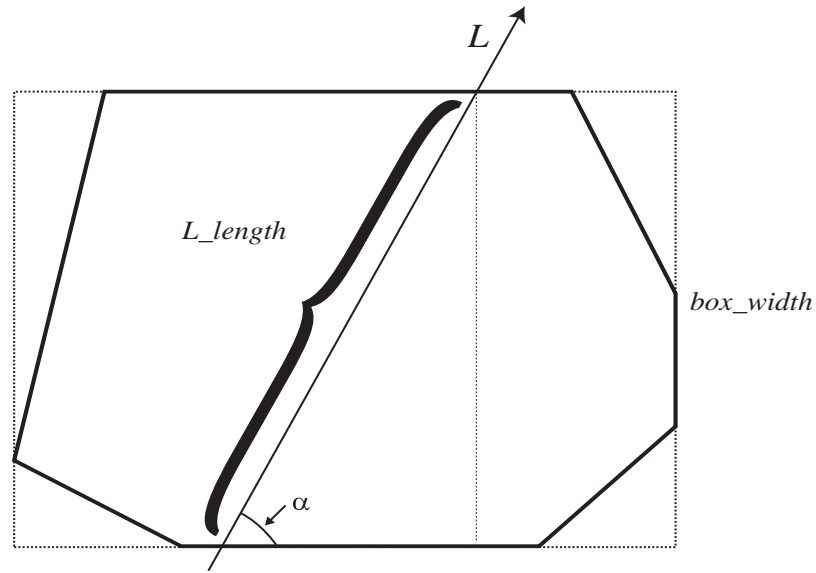$$s = \frac{L\_physical}{L\_pixel} \quad (\text{ft / pixel}) \,. \tag{9}$$

This will play a key role in the next step.

3.3 DISTANCE AND SPEED ESTIMATION

Next, we estimate the travel distance between frames and the vehicle speed using the scale factor just obtained from the above geometric analysis.

First, some assumptions are made:

a) Distance traveled by a car is defined by the displacement of its centroid.

b) Scale change is smooth (linear with pixel distance) along the camera focus. Therefore, all scale changes form an equal difference sequence.

c) Scale is homogeneous (constant) inside the car (box), so that the scale obtained from the ratio of the two lengths is equal to the scale factor at the centroid.
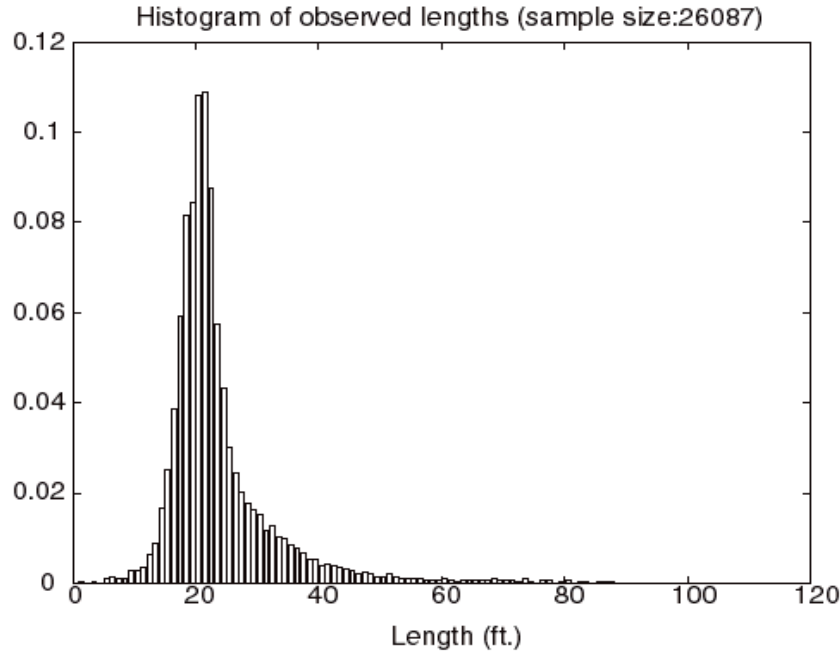
Figure 3.3 Vehicle length histogram

To obtain the physical distance of moving centers, we estimate the scale factors at each pixel along the travel path having angle α. To this end, we first need to compute the total number of pixels along the travel path, which can be obtained by using

$$\text{\# of pixels along moving angle } \alpha = \frac{\text{\# of vertical pixels}}{\sin \alpha} \quad , \tag{10}$$

where the number of vertical pixels is simply the vertical pixel length between the first and the last centroids.

For an image sequence with k frames, where s_1 is the scale factor at the centroid of the convex hull of the vehicle of interest in the first frame, s_k is the scale factor at the centroid of the convex hull of the vehicle in the k-th frame, and the number of pixels along the driving path between these two centroids is n, we can compute the scale change per pixel, Δs, as

$$\Delta s = \frac{(s_k - s_1)}{(n-1)} \quad (\text{ft} / \text{pixel}^2) . \tag{11}$$

The total distance D traversed between the images is then obtained by summing up the scale factor series as

$$D = ns_1 + \frac{n(n-1)}{2}\Delta s \quad \text{(ft)}$$
$$= n\frac{\left(s_1 + s_k\right)}{2}$$

(12)

The speed is then estimated as the ratio of the interframe travel distance and the known frame rate.

The material just presented is the first published algorithm for an estimate of single vehicle speed using a statistical vehicle length and an uncalibrated camera. The algorithm creates scale information on the fly from information contained in the image and does not require calibration markers in the physical environment.

The algorithm presented here is validated against ground truth measurements in the next chapter.

4 Field Trials and Discussions

4.1 FIELD TRIALS METHODOLOGY

To test our algorithm, we compared the distance estimates (called estimated distance) obtained with our dynamic calibration technique with ground truth measurements on the freeway. Because the travel time interval is set by the inter-frame time, the only unknown is the ground truth travel distance. Field trials used both the distance between and the size of the center stripes. Both these measurements are published by WSDOT, as seen in Appendix A.

4.2 EXPERIMENTAL RESULTS

Through extensive trials we tested the presented algorithm under different lighting conditions. Estimation error is defined as the difference of the ground truth distance and the estimated distance divided by the ground truth distance. Figure 4.1 shows the estimation error values and estimation error histogram for 60 image sequences. As suggested by Worrall et al [9], the mean car length, L_m, of 25.63 ft. is used in scale factor computations. The average estimation error for these 60 sequences is 8.7 percent.
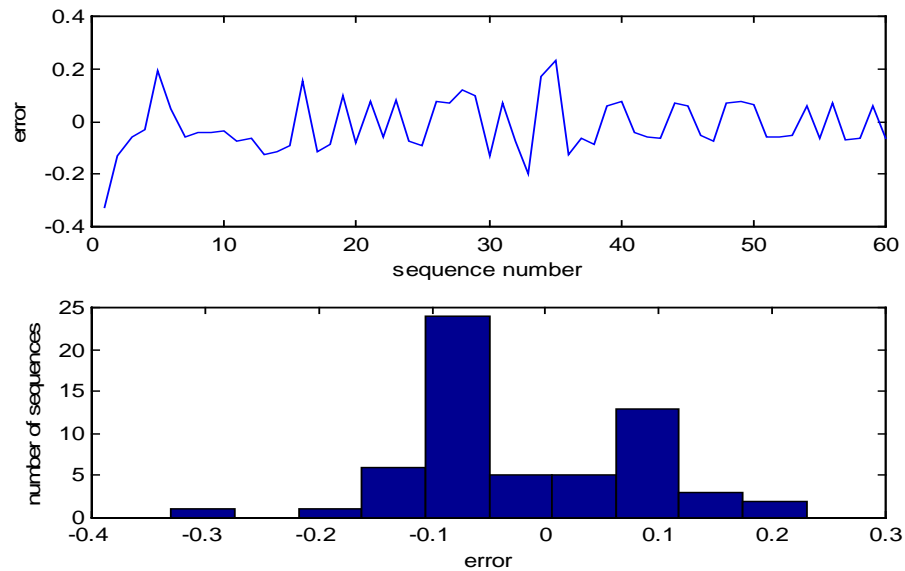

Figure 4.1 Errors and error histogram for 60 image sequences

Experiments suggested that when the area of shadow created by a vehicle is larger than two thirds of the vehicle area in the image, the estimation errors of our algorithm are unacceptable. We call this situation the severe shadow effect. Twenty such sequences were tested. The estimation error histogram is shown in Figure 4.2. Most produced estimation errors over 15 percent, some even over 25 percent. A typical image sequence with serious shadow effects is shown in Figure 4.3. Figure 4.4 shows two moving edge images for two frames in this sequence, where many moving edges actually represent the edges of shadows rather than those of the original vehicles. Initial analysis indicated that shadows will affect the reliability of the moving edge detection, the convex hull extraction, and, finally, the scaling computation, thereby distorting the distance and speed estimation. Without a priori knowledge of shadow shapes and directions, the effect of shadows cannot easily be included in this algorithm.
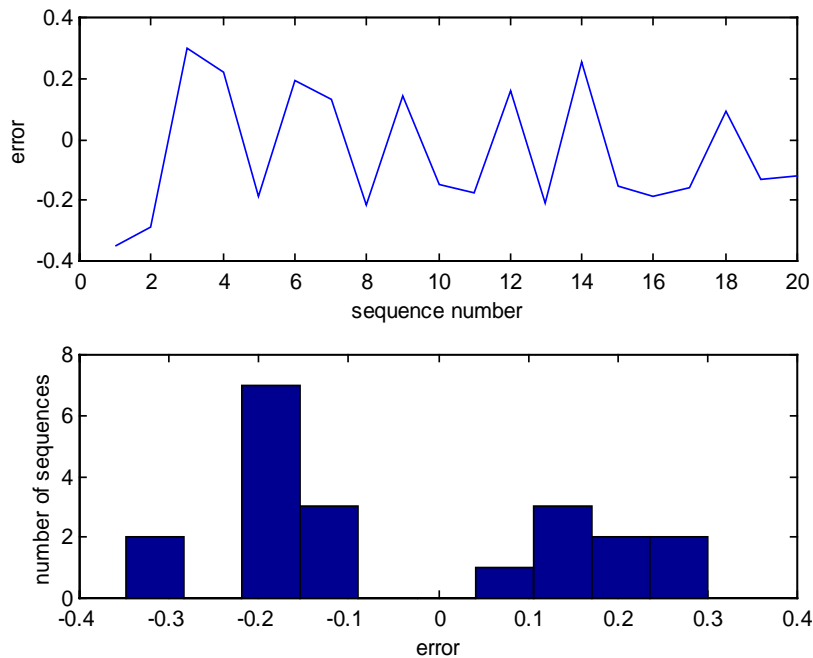
Figure 4.2 Errors and error histogram for 20 image sequences with severe shadow effects

Quantitative analysis of shadow effects is one focus for future improvements to the algorithm.

first frame

second frame

third frame

fourth frame

Figure 4.3 A typical sequence with severe shadow effects

Moving edges for the first frame
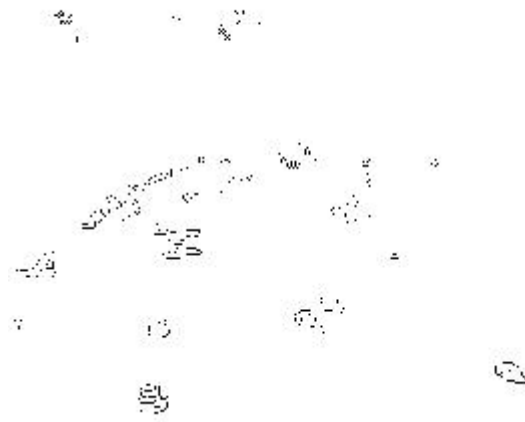
Moving edges for the fourth frame

Figure 4.4 Moving edges

4.3 ERROR ANALYSIS

From Worrall et al [9], the random variable vehicle length, $L\_physical$ (L is used below for simplicity), can be expressed as its expected value L_m (mean) and some deviation ΔL, that is

$$L = L_m + \Delta L \ .$$

(13)

For an image sequence with k frames, suppose L_1 is the car pixel length in the first frame and L_k is the car pixel length in the k-th frame. Consider a case in which the cars are moving away

from the camera, so that the scale factor increases with the distance from the camera. (The analysis is similar for a case in which the cars are moving toward the camera.) Combining equations (9) and (12) gives us the estimated distance D_m,

$$
\begin{aligned}
D_m &= \frac{n}{2}\left(\frac{L_m}{L_1} + \frac{L_m}{L_k}\right) \\
&= L_m \frac{n}{2}\left(\frac{1}{L_1} + \frac{1}{L_k}\right)
\end{aligned}
\tag{14}
$$

Considering length deviation in equation (13) gives us the deviated distance D_{de} as

$$
D_{de} = (L_m + \Delta L)\frac{n}{2}\left(\frac{1}{L_k} + \frac{1}{L_1}\right).
\tag{15}
$$

Let e be the absolute error of distance measurement, and thus $e = D_{de} - D_m$. Combining equations (14) and (15) gives the mean of error e,

$$
E\{e\} = \frac{n}{2}\left(\frac{1}{L_k} + \frac{1}{L_1}\right)E\{\Delta L\},
\tag{16}
$$

where $E\{*\}$ is the expected value operator, and the variance, $\mathrm{Var}\{e\}$, is

$$
\mathrm{Var}\{e\} = \left[\frac{n}{2}\left(\frac{1}{L_k} + \frac{1}{L_1}\right)\right]^2 \mathrm{Var}\{\Delta L\}.
\tag{17}
$$

Equations (16) and (17) reveal that the length deviation (L) directly affects the measurement error, since the pixel number n and pixel lengths L_k and L_1 are uniquely determined for a specific image sequence with k frames.

4.4 Possible System Extensions

The speed information obtained from this work can be used directly for many applications, such as traffic congestion detection. It is also worthwhile to note that with some modifications, our method can be readily extended to other traffic analysis, including incident detection, traffic model verification, and travel time estimation. The techniques introduced in this report can be used as a

basis for developing general-purpose, advanced intelligent traffic surveillance systems. For example, combined with character pattern recognition process, our method can be extended to recognize the vehicle license plate number, which has recently become an active research area.

5 Conclusion

There are many challenging problems in studying real traffic scenes within a complex background. In this report, efficient image processing techniques are applied to traffic analysis to estimate travel speed from image sequences of moving vehicles. Simple geometric relations are obtained directly from the image itself and are used to deal with real-world problems without explicit camera calibration. Furthermore, the techniques presented are validated against ground truth by field trials. Error analysis is also given in detail. The car length distribution is shown to be a key factor in the accuracy of speed sensing.

Some problems remain to be solved, including the effect of shadows and occlusion of vehicles.

As a result of the work presented here, a manuscript has been submitted to the IEEE Intelligent Transportation Systems Council for presentation at ITSC'99, a peer reviewed conference. A copy of this manuscript appears in Appendix B.

References

1. Kilger, M. Video-Based Traffic Monitoring. *International Conference on Image Processing and its Applications*, 7-9 April 1992, Maastricht, Netherlands, pp. 89-92.

2. Fathy, M. and M.Y. Siyal. An Image Detection Technique Based on Morphological Edge Detection and Background Differencing for Real-Time Traffic Analysis. *Pattern Recognition Letters*, Vol. 16, No. 12, December 1995, pp. 1321-1330.

3. Hoose, N. and L.G. Willumsen. Automatically Extracting Traffic Data From Videotape Using The CLIP4 Parallel Image Processor. *Pattern Recognition Letters*, Vol. 6, No. 3, August 1987, pp. 199-213.

4. Ali, A.T. and E.L. Dagless. Computer Vision for Automatic Road Traffic Analysis. *ICARCV 90, Proceedings of the International Conference on Automation, Robotics and Computer Vision*, 19-21 September 1990, pp. 875-879.

5. Fathy, M. and M.Y.Siyal, Real-Time Image Processing Approach to Measure Traffic Queue Parameters. *IEE Proceedings - Vision, Image and Signal Processing*, Vol.142, No.5, October 1995, pp. 297-303.

6. Soh, J., B.T. Chun, and M. Wang. Analysis of Road Sequences for Vehicle Counting. *1995 IEEE International Conference on Systems, Man and Cybernetics*, Vol.1, 22-25 October 1995, Vancouver, British Columbia, Canada, pp. 679-683.

7. Zifeng, J. Macro and Micro Freeway Automatic Incident Detection(Aid) Methods Based on Image Processing. *IEEE Conference on Intelligent Transportation Systems*, 9-12 November 1997, Boston, Massachusetts, USA, pp.344-349.

8. Picton, P.D. Tracking and Segmentation of Moving Objects in a Scene. *Third International Conference on Image Processing and its Applications (Conf. Publ. No.307)*, 18-20 July 1989, Warwick, UK, pp. 389-393.

9. Worrall, A.D., G.D. Sullivan, and K.D. Baker. A Simple, Intuitive Camera Calibration Tool for Natural Images. *Proceedings of the 5th British Machine Vision Conference*, 13-16 September 1994, York, UK, pp. 781-790.

10. Dickinson, K.W. and R.C. Waterfall. Video Image Processing for Monitoring Road Traffic. *IEE International Conference on Road Traffic Data Collection*, 5-7 December 1984, pp. 105-109.

11. Ashworth, R., D.G. Darkin, K.W. Dickinson, M.G. Hartley, C.L. Wan, and R.C. Waterfall. Applications of Video Image Processing for Traffic Control Systems. *Second International Conference on Road Traffic Control*, 14-18 April 1985, London, UK, pp. 119-122.

12. Takaba, S., M. Sakauchi, T. Kaneko, B. Won-Hwang, and T. Sekine. Measurement of Traffic Flow Using Real Time Processing of Moving Pictures. *32nd IEEE Vehicular Technology Conference*, 23-26 May 1982, San Diego, California, USA, pp. 488-494.

13. Hashimoto, N., Y. Kumagai, K. Sakai, K. Sugimoto, Y. Ito, K. Sawai, and K. Nishiyama. Development of an Image-Processing Traffic Flow Measuring System. *Sumitomo Electric Technical Review*, No. 25, January 1986, pp. 133-137.

14. Houkes, Z. Measurement of Speed and Time Headway of Motor Vehicles with Video Camera and Computer. *Proceedings of the 6th IFAC/IFIP Conference on Digital Computer Applications to Process Control*, 14-17 October 1980, Dusseldorf, West Germany, pp. 231-237.

15. Dailey, D.J. A Statistical Algorithm for Estimating Speed from Single Loop Volume and Occupancy Measurements. *Transportation Research B*, Vol. 33B, No. 5, June 1999, pp. 313-22.

16. Hoose, N. and L.G. Willumsen Real Time Vehicle Tracking Using the CLIP4 Parallel Processor. *Seminar on Information Technology in Traffic and Transport*. PTRC. Summer Annual Meeting, University of Bath, UK, 1987, pp. 113-131.

17. Koller, D., J. Weber, and J. Malik. *Robust Multiple Car Tracking with Occlusion Reasoning, Report No. UCB/CSD 93/780*, Computer Science Division (EECS) UC-Berkeley, 22 November 1993

18. Pratt, William K. *Digital Image Processing, 2nd Ed*. John Wiley and Sons. Inc., New York, c1991.

19. Davies, E.R. *Machine Vision: Theory, Algorithms, Practicalities*. 2nd Edition. Academic Press, London, England, 1997.

20. Ritter, Gerhard X. and Joseph N. Wilson. *Handbook of Computer Vision Algorithms in Image Algebra*. CRC Press, Boca Raton, Florida, 1996.

21. Gil, S., R. Milanese, and T. Pun. Comparing Features for Target Tracking in Traffic Scenes. *Pattern Recognition*, Vol. 29, No. 8, August 1996, pp. 1285-1296.

22. Kudo, Y., T. Yamahira, T. Tsurutani, and M. Naniwada. Traffic Flow Measurement System Using Image Processing. *33rd IEEE Vehicular Technology Conference*, Toronto, 25-27 May 1983, Ontario, Canada, pp. 28-34.

23. Cai, Q., A. Mitiche, and J.K. Aggarwal. Tracking Human Motion in an Indoor Environment. *International Conference on Image Processing*, 23-26 October 1995, Washington, D.C., USA, Vol. 1, pp. 215-218.

24. Vieren, C., F. Cabestaing, and J.G. Postaire. Catching Moving Objects with Snakes for Motion Tracking. *Pattern Recognition Letters*, Vol. 16, No. 7, July 1995, pp. 679-685.

25. Serra, Jean Paul. *Image Analysis and Mathematical Morphology*. Academic Press, London, New York, 1982.

26. Fathy, M. and M.Y. Siyal. A Window-Based Edge Detection Technique for Measuring Road Traffic Parameters in Real-Time. *Real-Time Imaging*, Vol. 1, No. 4, October 1995, pp. 297-305.

27. Stewart, B.D., I.A.D. Reading, M.S. Thomson, C.L. Wan, and T.D. Binnie. Directing Attention for Traffic Scene Analysis. *Fifth International Conference on Image Processing and its Applications*, 4-6 July 1995, Edinburgh, UK, pp. 801-805.

28. Bevington, Philip R. *Data Reduction and Error Analysis for the Physical Sciences*. McGraw-Hill Book Company, New York, 1969.

Appendix A

WSDOT Lane Stripe DATA

Skip Center Stripe

No Pass Stripe
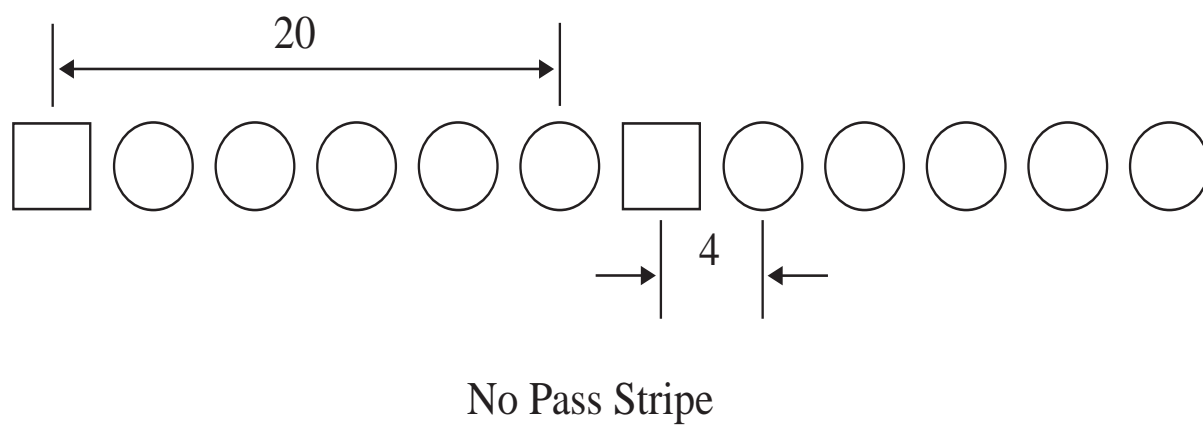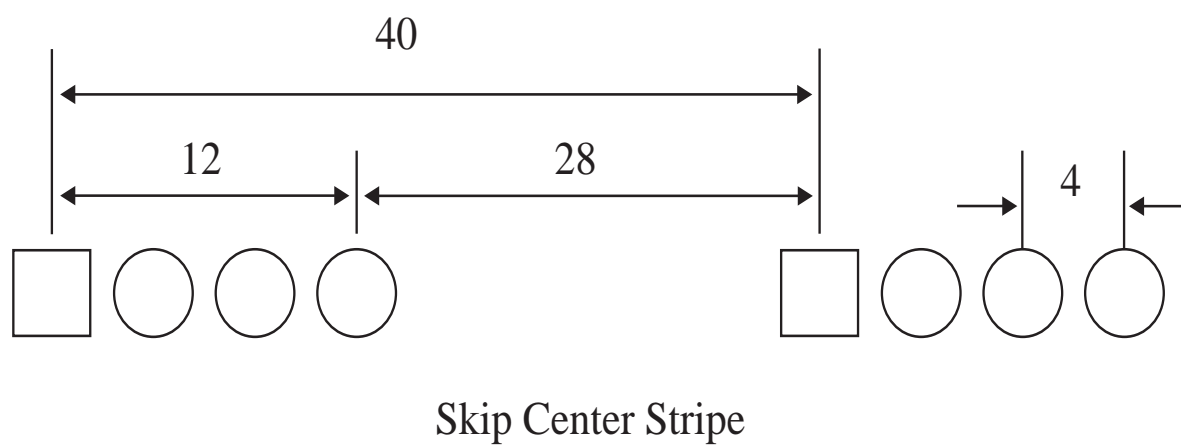
Appendix B

Copy of manuscript submitted to IEEE Intelligent Transportation Systems Council for presentation at ITSC'99.

An Algorithm to Estimate Vehicle Speed Using Un-Calibrated Cameras

D.J. Dailey, L. Li
Department of Electrical Engineering
Univeristy of Washington
Seattle, Washington, 98195

Abstract

In this paper we present a new algorithm to estimate speed using a sequence of video images from an un-calibrated camera. The algorithm uses frame differencing to isolate moving edges and track vehicles between frames. The algorithm uses a known vehicle length distribution with image information to estimate speed.

1 Introduction

Image processing techniques have been applied to traffic scenes for a variety of purposes including: queue detection, incident detection, vehicle classification, and vehicle counting [1, 2, 3, 4, 5, 6]. In this paper, we present a new algorithm to estimate speed using a sequence of video images from an un-calibrated camera. This work is motivated by the large number of roadside cameras installed by DOT's to observe traffic. The cameras are typically not installed in a manner that they can easily be calibrated, and they are typically used by operators who can tilt, pan, and zoom using a joystick to change the camera calibration. The combination of movable cameras and lack of calibration makes estimating speed for un-calibrated cameras a challenge.

Relatively few efforts have been made to measure speed using video images from un-calibrated cameras. Some preliminary research on pixel speed estimation in images appears in [5]. In previous work few efforts were made to map pixel speed to ground truth speed. A review of the literature on speed estimation using cameras indicates that most algorithms either use reference information in the scene or create such references interactively. For example, Worrall [7] reports an interactive tool to perform camera calibration in which an operator uses parallel road marks to identify vanishing points and then places a rectangular calibration grid on the image. Further, in [8] and [9], speed measurements are made using the known physical distance between two detection windows placed on the

road image by an operator. Similarly, several other authors [10, 11] suggest estimating speed by placing two detection lines, of known separation, in the image and measuring travel times between the lines. In addition, Houkes [12] suggest the selection of 4 reference points forming a rectangle and performing off-line measurements. All these methods require the operator to perform a calibration procedure before speed estimation can be undertaken.

In this paper, it is assumed that we have no control over camera movements, and thus cannot directly obtain information such as camera focus, tilt, or angle. It is further assumed that the camera parameters can change with time. In the work presented here, we are monitoring congested freeways and have neither the ability nor the authority to set permanent marks on the road. Given this scenario, we believe on-line calibration is a necessary step to enable the use of the large, installed base of TMS cameras.

We assert that exact calibration is not necessary to estimate speed. Instead, we use: (1) geometric relationships inherently available in the image, (2) some common sense assumptions (listed below) that reduce the problem to a 1-D geometry, and (3) the distribution of vehicle lengths, to propose a novel method that extracts scale information and estimates speed.

To describe and demonstrate our speed estimation scheme, we first review the assumptions made in formulating the algorithm. We then enumerate the steps of the algorithm, followed by a discussion of the individual steps. Finally we present some preliminary quantitative results of the algorithm.

2 Underlying Assumptions

To create an algorithm to estimate speed from video images we make several assumptions to simplify the problem:

1. The speed of the vehicles is finite. The speed of a vehicle has both physical and legal limits.

2. The vehicle movement is smooth. There are no sudden changes of direction in the time interval (330ms) between frames in the image sequence.

3. Motion is constrained to the road plane. Tracking of vehicles in the image sequence is a one dimensional problem.

4. The scale factor (feet per pixel) varies linearly along the direction of vehicle travel. This assumption constrains the vehicles to be moving generally toward or generally away from the camera.

5. The lengths of the vehicles in the images are realizations from a known vehicle length distribution.

With these assumptions, the vehicles are treated as though they travel in one dimension along a straight line in the image. The vehicles are tracked across these images to obtain scale factors that estimate the real-world distance represented by pixels at various locations in the image. Using a linear function to fit to the empirical scale factors it is possible to estimate the real-world distance traveled. Combining the distance traveled with the known frame rate allows us to estimate speed. An algorithm to perform this estimation is presented in the next section.

3 The Algorithm

The algorithm operates on a series of at least five sequential images. The inner loop operates on sequential groups of three images to create one enhanced image. The outer loop uses a sequence of enhanced images to estimate speed.

Outer Loop

1. Obtain five or more sequential images (320x240), gray scale at three frames per second (e.g. $[I_i, I_{i+1}, I_{i+2}, I_{i+3}, I_{i+4}, ..., I_{i+N}]$ where $N \geq 5$)

2. Create sets of three sequential images (e.g. $[I_i, I_{i+1}, I_{i+2}]$ is the ith set of $(N-2)$ sets)

   Inner Loop

   For each of the sets of three sequential video images, perform the following:

   (a) Median filter each image.

   (b) Difference the first and second images $((I_i - I_{i+1}))$ as well as the third and second images $(I_{i+2} - I_{i+1}))$ to get two difference images.

   (c) Apply a Sobel edge detector to the difference images to obtain edge images $Sobel(I_{i+2} - I_{i+1})$ and $Sobel(I_i - I_{i+1})$.

   (d) Threshold the edge images to create binary images.

   (e) Intersect the two binary images to obtain the moving edge image $(ME(I_{i+1}))$ for the I_{i+1} image:

   $$ME(I_{i+1}) = \quad Threshold(Sobel(I_{i+2} - I_{i+1}))$$
   $$\cap \quad Threshold(Sobel(I_i - I_{i+1})).$$

   (f) Apply dilation to the moving edge image.

   (g) Apply erosion to the moving edge image.

   (h) Identify the set of points $\mathbf{C}_j(I_{i+1})$ for the j convex hulls in the moving edge image $ME(I_{i+1})$.

   (i) Calculate centroid $\rho(i+1, j) = (x, y)$ for the jth convex hull in image I_{i+1}.

   (j) Calculate the set of points for the bounding boxes $\mathbf{B}_j(I_{i+1})$ for the j convex hulls.

   End of the inner loop

3. Select sets of co-linear centroids $[\rho(i+1, j), \rho(i+2, j), \rho(i+3, j), \quad ... \quad \rho(N-2, j)]$ in sequential images and estimate a best fit line through these points. The slope of this line is the tangent of the angle of motion α for the jth centroid in the series of images. This is used to establish a new coordinate, z, along the direction of motion such that $z^2 = x^2 + y^2$ and $tan(\alpha) = dy/dx$.

4. For each of the collinear bounding boxes in sequential images, estimate the pixel length $L(i+1, j)$ along the direction α using [1]
   $$\frac{sup(y : y \in \mathbf{B}_j(I_{i+1})) - inf(y : y \in \mathbf{B}_j(I_{i+1}))}{\sin \alpha}.$$

5. Estimate the scale factor q (feet/pixel) for the z location of the centroid $\rho(i+1, j)$ using the mean vehicle length $\bar{l}$,

   $$\hat{q}(i+1, z) = \frac{\bar{l}}{L_p(i+1, j)}.$$

6. Using a series of two or more scale factor estimates, estimate the slope (m) and intersection (b) of the scale factor function $q(z|m, b)$ using

   $$\min_{(m,b)} \|q(z|m, b) - \hat{q}(i+1, z)\| \quad \forall i,$$

   where $q(z|m, b) = mz + b$, and z is the distance along a line at an angle α in the images.

   ---
   [1] sup is the *supremum* or *least upper bound* and inf is the *infimum* or *greatest lower bound* [13]

7. Estimate the interframe distances,

$$d_k = \int_{z_k}^{z_{k+1}} q(z)dz \qquad \forall \quad k \in (i+1, N-2).$$

8. Estimate the mean of interframe distances, $E[d_k]$, and use the ratio of the interframe mean and the frame rate (Δt) to estimate speed,

$$\hat{S} = \frac{E[d_k]}{\Delta t}.$$

End Outer Loop

4   Algorithm Operation

To explain the operation of the algorithm just enumerated, we identify the basic tasks necessary to estimate speed from sequential un-calibrated images and map these tasks into the steps in the algorithm. The tasks necessary to obtain speed from un-calibrated images are: (1) obtain sequential images, (2) identify the moving vehicles in the sequential images, (3) track the vehicles between images, (4) dynamically estimate the scale factor in feet per pixel, and (5) estimate speed from distance traveled and the interframe delay.

As mentioned earlier, the algorithm operates on sets of sequential images taken from DOT CCTV cameras. The images used in this work are, grey scale, 320 by 240 pixels, sampled three times per-second. The resolution and sample rate are selected to provide sufficient detail in the image to identify individual vehicles and to capture sequential images rapidly enough so that individual vehicles can be tracked between images without pattern recognition techniques (e.g. the vehicles moves no more that about one vehicle length between images).

The images used in our algorithm are taken from roadside CCTV cameras installed by Washington State DOT in their traffic management role. The DOT transports the video from the roadside cameras to the control center using a dedicated fiber system. In the control center, operators can pan, tilt, and zoom the cameras using a joystick. The cameras are actively being used for traffic management activities. No camera calibration information is available for these cameras, and it is the purpose of this work to demonstrate that the images from such cameras can be used as an alternative speed estimate

The video is digitized at a rate of three-frames per second and stored in files using the Jpeg image format. These Jpeg files are the sequential images required for step one in the outer loop of the algorithm. Sets of three sequential images are used in the inner loop of the algorithm. The left side of Figure 1 shows two example images.

In step (b) of the algorithm, a median filter, using a 3x3 kernel, is applied to each image to remove high frequency noise in the images [14, 15].

To identify the moving vehicles in the images, the non-moving background must be removed. Two basic techniques to remove the static background information appear in the literature. The first is to obtain a frame with only the background that can be subtracted from the frames in which there are vehicles [16]. This frame is then updated to match the current lighting levels [2]. This method is not only computationally expensive, but it may be impossible, on congested freeways, to obtain an image with the correct lighting level and with no vehicles present. The second technique uses sequential frames to perform forward and backward differences between the frames [17, 16, 18]. Vieren [18] suggests using interframe differences with a differential operator to extract moving edges.

The algorithm presented here uses interframe differences and then applies a Sobel edge detector to the resulting image. Step (d) of the algorithm creates two difference images, and step (e) applies the Sobel edge detector to those images. The resulting images are thresholded to obtain a binary images. The upper right image in Figure 1 is the binary image that results of applying the Sobel edge detector to the difference of the two images in the left column of Figure 1. The two binary images are intersected in step (f) of the algorithm to obtain a moving edge image. The resulting moving edge image for the example sequence appears in the lower right of Figure 1.

Examining the lower right image in Figure 1 shows that while we have identified the moving edges, those edges do not make closed polygons identifiable as individual vehicles. To overcome this problem and create closed curves, we use two morphological operations. We enhance the moving edge image by sequentially applying dilation and erosion. [19] Dilation of an object is the translation of all of its points with regard to a structural element followed by a union operation. Dilation is applied to the binary image to close the curves in the moving edge image; it also expands the overall size of the area enclosed. Erosion is then used to shrink the object back to the original size. In the algorithm presented, a 3x3 structural element is used in step (f) to perform dilation and in step (g) to perform erosion.

After the application of the morphological operators, the moving edges are filled in to create moving
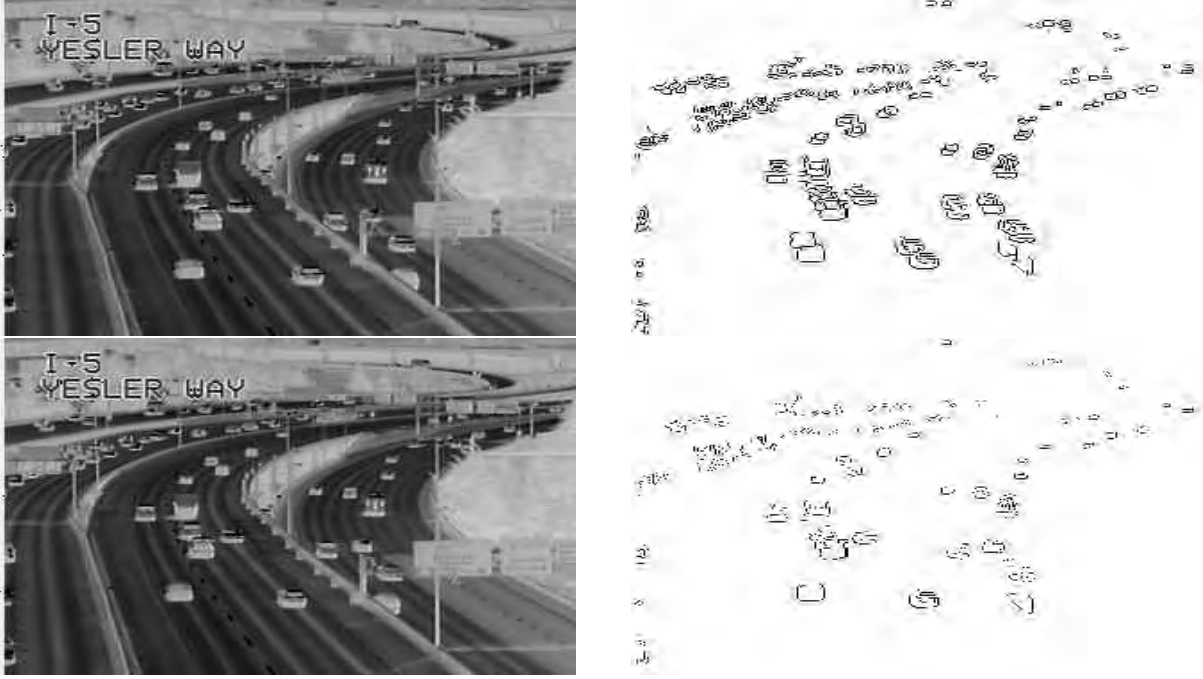
Figure 1: Typical image sequence (left). Sobel edges in the difference image (right top). Moving edge image for the bottom right image created by intersecting difference images. intersecting (right bottom).

blobs. These moving blobs represent the vehicle motion in the images. Past work has asserted that the convex hull surrounding a vehicle in an image is a good approximation of the projection of a vehicle in the image [20]. To characterize the moving blobs, we first calculate the convex hull for the blobs in step (h) of the algorithm. We also calculate the centroid of the convex hulls in step (i). The centroids of the convex hulls are used as the effective location of the vehicle in the image.

Having located a vehicle in one image, the vehicle is tracked across images by enforcing co-linearity of the centroids of the convex hulls. The left side of Figure 2 presents a representation of three convex hulls with centroids $(x_1, y_1), (x_2, y_2), (x_3, y_3)$. In step (3) of the algorithm, the vehicle is tracked as moving along the line at an angle (α) relative to the horizontal scan lines in the image. In the work presented here, a minimum value of 0.90 of the linear regression correlation coefficient,

$$
r = \frac{n \sum_{i=1}^{n} x_i y_i - \sum_{i=1}^{n} x_i \sum_{i=1}^{n} y_i}{(n \sum_{i=1}^{n} x_i^2 - (\sum_{i=1}^{n} x_i)^2)^{1/2} (n \sum_{i=1}^{n} y_i^2 - (\sum_{i=1}^{n} y_i)^2)^{1/2}},
$$

(1)

is used to identify co-linear centroids and track a vehicle. This completes tasks one through four necessary to estimate speed.

The fifth task necessary to estimate speed is to make an estimate of the scale factor that maps distance traveled in the image to distance traveled on the road. We have assumed the vehicles are taken from a known distribution [21], and we can use the properties of that distribution to estimate the length of the vehicles in the images. We make individual estimates of the scale factor $(\hat{q})$ as the ratio of the mean vehicle length $(\bar{l})$, taken from the known distribution, and the estimate of vehicle length from the image. This latter length is approximated by the length of the line, in the direction of travel, crossing the bounding box surrounding the convex hull of the vehicle. The right side of Figure 2 illustrates this approximation, and step 4
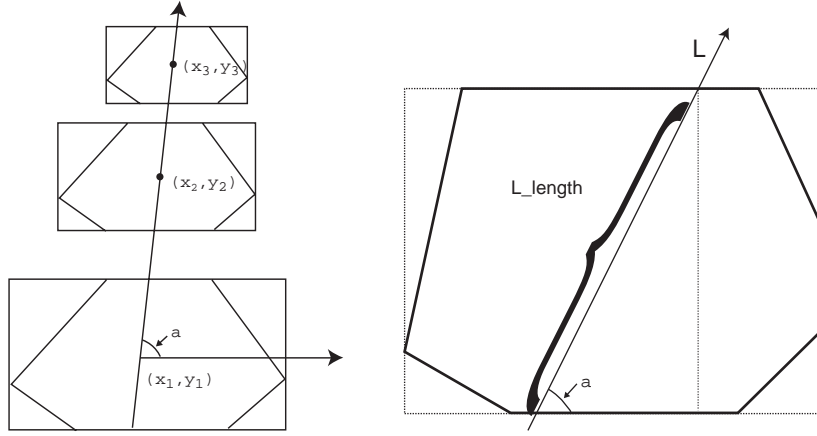
Figure 2: Use of centroids to establish the travel direction α (left), Use of bounding box to estimate vehicle length (right).

in the algorithm provides this estimate.

We assume that the scale factor q changes linearly along the path that the vehicle travels,

$$q(z|m,b) = mz + b, \qquad (2)$$

where z is the distance along a line at an angle α in the images. The parameters of this scale factor function are estimated in step 6 of the algorithm using the set of scale factor estimates from step 5. The distance traveled is the integral of this function along the z direction,

$$d = \int_{z_1}^{z_2} q(z)dz. \qquad (3)$$

This distance is estimated in step 7 of the algorithm.

Finally, having an estimate of the distance traveled, we use the interframe sample time in step 8 to estimate the vehicle speed,

$$\hat{S} = \frac{E[d_k]}{\Delta t}. \qquad (4)$$

This provides an estimate of speed from un-calibrated cameras.

5   Empirical Results

This paper presents preliminary results of applying the algorithm to images from a variety of lighting conditions. Figure 3 is a histogram of the error between the individual speed estimates and the ground truth. These results are for 60 tests of the algorithm without regard to lighting effects. There are errors as large as 30% in one of the tests. On examining the relationship between lighting conditions and the error in the

estimates it has become clear that the shadow effects may account for the errors of over 10% in the speed estimate. Reconsiling the algorithms against lighting conditions is an ongoing effort.

This paper presents a new algorithm to estimate speed from un-calibrated cameras. Un-calibrated cameras are widely available to DOT operators and can provide a valuable, additional quantitative measure for traffic operations and traveler information.

Acknowledgments

References

[1] M. Kilger, "Video-Based Traffic Monitoring," in *International Conference on Image Processing and its Applications*, 7-9 April 1992, Maastricht, Netherlands.

[2] M. Fathy and M.Y. Siyal, "An Image Detection Technique Based on Morphological Edge Detection and Background Differencing for Real-Time Traffic Analysis ," *Pattern Recognition Letters*, vol. Vol. 16, No. 12, pp. 1321–1330, 1995.

[3] N. Hoose and L.G. Willumsen, "Automatically Extracting Traffic Data From Videotape Using The CLIP4 Parallel Image Processor ," *Pattern Recognition Letters*, vol. Vol. 6, No. 3, pp. 199–213, 1987.

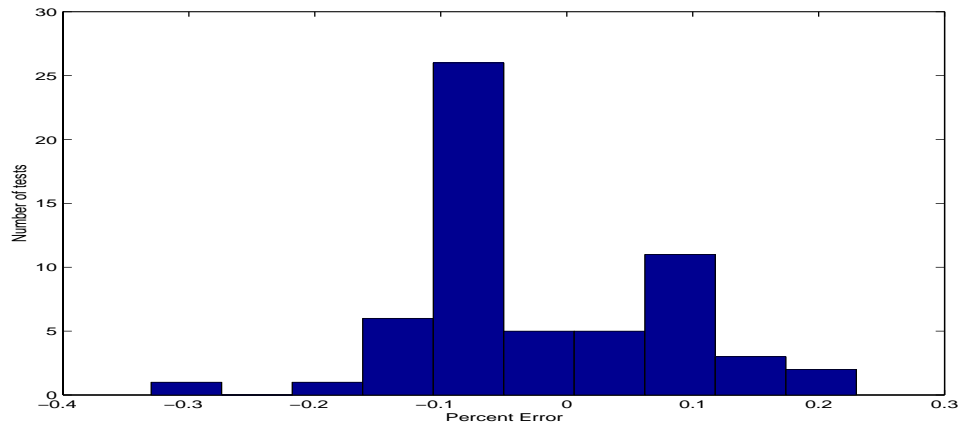[4] A.T. Ali and E.L. Dagless, "Computer Vision for Automatic Road Traffic Analysis," in *ICARCV*

Figure 3: Histogram of percent error.

90, *Proceedings of the International Conference on Automation, Robotics and Computer Vision*, 19-21 September 1990.

[5] B.T. Chun Soh, J. and M. Wang, "Analysis of Road Sequences for Vehicle Counting ," in *1995 IEEE International Conference on Systems, Man and Cybernetics Vol.1*, 22-25 October 1995, Vancouver, British Columbia, Canada.

[6] J. Zifeng, " Macro and Micro Freeway Automatic Incident Detection(Aid) Methods Based on Image Processing," in *IEEE Conference on Intelligent Transportation Systems*, 9-12 November 1997, Boston, Massachusetts, USA.

[7] G.D. Sullivan Worrall, A.D. and K.D. Baker, "A Simple, Intuitive Camera Calibration Tool for Natural Images ," in *Proceedings of the 5th British Machine Vision Conference*, 13-16 September 1994, York, UK.

[8] K.W. Dickinson and R.C. Waterfall, "Video Image Processing for Monitoring Road Traffic ," in *IEE International Conference on Road Traffic Data Collection*, 5-7 December 1984.

[9] D.G. Darkin K.W. Dickinson M.G. Hartley C.L. Wan Ashworth, R. and R.C. Waterfall, " Applications of Video Image Processing for Traffic Control Systems," in *Second International Conference on Road Traffic Control*, 14-18 April 1985, London, UK.

[10] M. Sakauchi T. Kaneko B. Won-Hwang Takaba, S. and T. Sekine, "Measurement of Traffic Flow Using Real Time Processing of Moving Pictures ,"

in *32nd IEEE Vehicular Technology Conference*, 23-26 May 1982, San Diego, California, USA.

[11] Y. Kumagai K. Sakai K. Sugimoto-Y. Ito K. Sawai Hashimoto, N. and K. Nishiyama, " Development of an Image-Processing Traffic Flow Measuring System," *Sumitomo Electric Technical Review*, vol. No. 25, pp. 133–137, 1986.

[12] Z Houkes, "Measurement of Speed and Time Headway of Motor Vehicles with Video Camera and Computer ," in *Proceedings of the 6th IFAC/IFIP Conference on Digital Computer Applications to Process Control*, 14-17 October 1980, Dusseldorf, West Germany.

[13] D.G. Luenberger, *Optimization by Vector Space Methods*, John Wiley & Sons, Inc., 1969.

[14] William K Pratt, *Digital Image Processing* , John Wiley and Sons. Inc., 2nd edition, c1991.

[15] E.R. Davies, *Machine Vision: Theory, Algorithms, Practicalities*, Acedemic Press, 2nd edition.

[16] A. Mitiche Cai, Q. and J.K. Aggarwal, "Tracking Human Motion in an Indoor Environment," in *International Conference on Image Processing, Vol. 1*, 23-26 October 1995, Washington, D.C., USA.

[17] T. Yamahira T. Tsurutani Kudo, Y. and M. Naniwada, "Traffic Flow Measurement System Using Image Processing ," in *33rd IEEE Vehicular Technology Conference*, 25-27 May 1983, Toronto, Ontario, Canada.

[18] F. Cabestaing Vieren, C. and J.G. Postaire, " Catching Moving Objects with Snakes for Motion Tracking," *Pattern Recognition Letters*, vol. Vol. 16, No. 7, pp. 679–685, 1995.

[19] Jean Paul Serra, *Image Analysis and Mathematical Morphology* , Academic Press, 1982.

[20] R. Milanese Gil, S. and T. Pun, "Comparing Features for Target Tracking in Traffic Scenes ," *Pattern Recognition*, vol. Vol. 29, No. 8, pp. 1285– 1296, 1996.

[21] D.J. Dailey, "A Statistical Algorithm for Estimating Speed from Single Loop Volume and Occupancy Measurements ," *Trans Research B*, 1999.